International Journal of Research in Engineering and Applied Sciences(IJREAS)
Available online at http://euroasiapub.org/journals.php
Vol. 7 Issue 6 , June-2017, pp. 249~264
ISSN (O): 2249-3905, ISSN(P): 2349-6525 | Impact Factor: 7.196

Spectral Studies of Transition Metal Ions (Mn2+, Cu2+, Zn2+) Doped CdS Nanoparticles Under Solvothermal Method

S.Rinu Sam

Sivaji College of Engineering and Technology, Manivila, Tamil Nadu, India.

Abstract

The microwave assisted solvothermal method was employed for the preparation of pure and doped CdS nanoparticles.The cadmium acetate and thioacetamide were used as the cadmium source and sulfide source with the solvent ethylene glycol. The transition metal ions doped Cds nanoparticles are have tremendous applications in optical light emitting diodes. The prepared pure and doped CdS nanocrystals were characterized by XRD, UV-VIS Absorbance, UV-VIS Transmittance and FTIR are recorded and discussed briefly.

Key words: Solvothermal, Thioacetamide, Nanoparticles, UV-VIS.

1. Introduction

The Cadmium Sulphide (CdS) is an important II–VI group semiconductor (Eg = 2.42 eV) with excellent physical and chemical properties, which has promising applications in multiple technical fields such as photochemical catalysis, gas sensors, detectors for fast laser and infrared, solar cells, nonlinear optical materials, various luminescence devices, optoelectronic devices etc. [1-7]. CdS is the most promising compound among II–VI group semiconductor for detecting visible radiation [8]. Using various methods CdS nanoparticles can be obtained [9-12]. Many papers are recently published about the synthesis of chalcagenides with the solvothermal method [12-24]. The elementary sulphur powder was normally used as the chalcogenide source and here we choose thioacetamide as the sulphide source. Because it is much easier for thioacetamide to release sulphide ions and it will be beneficial to lower the reaction temperature and shorten the reaction period. With all these compounds we choose the nontoxic, in corrosive ethylene glycol as the solvent and this is more favourable to the environment.

2. Experimental

The chemicals including Cadmium acetate ($Cd(CH_3COO)_2.2H_2O$), Thioacetamide (CH_3CSNH_2) and Ethylene glycol ($HOCH_2CH_2OH$) are the analytical reagents. In this present study ethylene glycol was used as the solvent. Cadmium acetate and Thioacetamide are mixed with ethylene glycol are added to an autoclave and the precursor materials were reacted with 800W domestic microwave oven for 20 minutes. During the process of synthesis, Thioacetamide (TAA) can react with the trace water containing in ethylene glycol and also the de-ionized water in cadmium acetate ($Cd(Ac)_2$) , and release H_2S gradually. It undergo thermal decomposition under microwave irradiation to produce Cadmium Sulphide (CdS).

$$CH3CSNH2 + 2H2O = CH3COONH4 + H2S$$

$$Cd(Ac)2 + H2S = CdS + 2HAc.$$

In this microwave synthesis, ethylene glycol and microwave irradiation play the key role for the preparation of CdS nanoparticles. Ethylene glycol acting as both reaction media and dispersion

media can efficiently absorb and stabilize the surface of the particles and can favour the production of CdS nanocrystals. The product of orange coloured CdS nanoparticles are separated from the mixtures by centrifugation, washed with de-ionized water for four times and then with alcohol for two times. This pure CdS sample was annealed at about 100 ºC for 120 minutes to get phase-pure nanoparticles of CdS and the sample is called Sample A.

In order to synthesize nanoparticles of doped CdS:Tm (Tm = Zn2+, Mn2+, Cu2+), chemicals such as zinc acetate, manganese acetate and copper acetate were taken as the precursor materials for doping. To obtain CdS:Zn2+, 1 mol%, 2 mol% and 3 mol% of zinc acetate separately were added to the solution of cadmium acetate ($Cd(Ac)_2$) and thioacetamide (TAA) and was kept in the microwave oven. It was further processed similar to the processing of undoped CdS nanoparticles as explained above. Similarly, to synthesize CdS:Mn2+, 1 mol%, 2 mol% and3 mol% of manganese acetate were used, to obtain CdS:Cu2+ nanoparticles,1 mol%, 2 mol%and 3 mol% of copper acetate were added separately to the solutions of cadmium acetate (Cd (Ac)2)and thioacetamide(TAA).

3. Result and Discussion

3.1 Powder XRD of Pure CdS nanoparticles

The as-prepared Pure CdS obtained by the solvothermal route in the present work were characterized by Powder X-ray Diffraction technique(XRD). The structure and phase purity of the powder were examined using an X-ray diffractometer (Model Bruker AXS D-8) with Nickel filtered Cu-Kα radiation (Cu Kα: λ = 1.5406 Å) with 2θ ranging from 10° to 80° at the speed of 2°min-1. The sample was deposited on the glass substrates. After the ethanol was volatilized, the sample was analyzed. Figure 1 shows the XRD pattern for pure CdS (100 ºC for120 minutes) nanocrystal sample, synthesized by solvothermal method using the microwave oven. The pure CdS sample is annealed at 100°C for 120 minutes.

In the figure 1 the XRD result of the sample A shows that the pure CdS nano crystals consists of cubic structure as well as little hexagonal structure. In the synthesis of colloidal CdS particles cubic CdS phase is most often, but the macro scale phase of CdS is normally with the hexagonal structure [13]. In solvothermal synthesis, the hexagonal phase is more common [24, 25]. The coexistence of cubic and hexagonal phases has also been reported [21] and we also obtain cubic phase as well as hexagonal phase in the present system. The grain size of the pure nanocrystalline CdS was calculated from the Scherrer's equation [21-24]. The Scherrer's formula is given by:D = $0.9\lambda/\beta Cos\theta$

Where D is the crystallite size in nm, λ is the wavelength of the X-rays (1.5406 Å), β is the full width at half maximum and θ is the diffraction peak angle. In this present study the particle size of the pure CdS nanoparticles is given by 16.65 nm. The 'hkl' values are compared with the standard JCPDS file (10-454) [12]. All the experimental values are given in the table 1.

3.2 Spectral studies

3.2.1 UV-Visible spectroscopic study of CdS, CdS:Tm (Tm = Zn2+, Mn2+, Cu2+)

To study the size-dependent quantum size effect and the optical quality of the pure CdS and CdS:Tm nanocrystals, optical absorption studies are carried out by ultrasonically dispersing the samples in spectroscopic grade ethanol. The room temperature ultraviolet-visible spectra of pure CdS and doped CdS:Tm samples were recorded, in the absorption mode and transmittance mode. The optical absorption spectrum of the Pure CdS nanocrystals synthesized in this work is depicted in

figure (2). The spectrum shows the characteristic blue shift and this blue shift can be explained as a quantum size effect, due to the electron-hole confinement in a small volume [26].The UV-absorption edge provides a reliable estimate of the band gap of any system. The band gap energy can be calculated from the equation

$$E = h\nu, \qquad \text{(a)} \qquad (\text{where}, h\nu = hc/\lambda)$$

$$E = hc/\lambda(1.6\times10\text{-}19),$$

$$\text{ie, } Eg = 1240/\lambda \qquad \text{(b)}$$

where h,ν and c are the constants and Eg is the band gap energy of the material.When allowed direct transition is pre-assumed, as usually done by other research workers, band gap energy may be obtained from extrapolation of the straight line portion of the (Abs) vs λ plot. The band gap energy was calculated by plotting the optical energy (Abs) against λ and is shown in figure (2 and 3).

From the figure (2) it is observed that in the infrared (IR) and near infrared (NIR) region it has a low absorption spectrum. The bulk Cds shows the peak at 515 nm in the visible region [27]. But, the spectra of sample exhibit absorption peak in the range of 505 nm. This peak is assigned to the optical transition of the first excitonic state and shifted gradually to the lower wavelength (blue shift) as the ratio ions increased. This shift may be due to the quantum size effects and as well as approve the formation of smaller particles [28, 29]. Consequently, the excitation of electrons from valance band to conduction band requires higher energy, which results in the blue shift or light absorption in higher energy region or lower wavelength region.

This blue-shift also confirms the nanocrystalline nature of the samples and is caused by the strong quantum size effect in nanoparticles. The absorption edge shifts towards lower wavelength side or blue region as the doping concentration is increased indicating that effective band gap energy increases with decreasing the particle size. In a semiconductor, the increase in band gap between the valence and conduction band results from the decrease in the particle size. It is found that the band gap of the pure CdS nanosystem in the present study is 2.45 eV and this value is found to be larger than that of bulk CdS. The bulk band gap of CdS is 2.42 eV [30]. It implies that the band gap energy of nanocrystalline CdS increases by 0.03 eV when compared to that of bulk CdS [31] and this increase in the band gap energy is due to quantum confinement of charge carriers in the CdS nanosystem[32]

The transmittance spectra of as prepared Cds nanoparticle is show in the figure(3).This spectra reveals that the nanoparticle grown under the same parametric condition have low absorbance in the visible and near infrared region and are high in the ultra violet region. The spectra of sample exhibit transmition peak in the range of 537 nm. It is found that the band gap of the pure CdS nanosystem using the above equation in the present study is 2.30 eV and this value is found to be smaller than that of bulk CdS. It implies that the band gap energy of nanocrystalline CdS decreases by 0.12 eV, when compared to that of bulk CdS [31]. Here it can be observed that band gap of the crystal decreases from 2.45ev to 2.30 ev when comparing with absorbance and transmittance mode. This variation of the band gap may be useful to design a suitable window material in fabrication for solar cells [33].

Figure (4) shows the overlay spectrum of CdS: Zn2+ (1 mol %, 2 mol % and 3 mol %). The absorption peak at 508 nm is blue shifted compared to the bulk CdS for which the absorption peak is at 515 nm [29]. The band gap energy of the doped samples are calculated by plotting the (abs) against λ and is shown in figure (4) and the obtained band gap energy values are given in table(2). It is evident from the values of the band gap energies for different ratio of CdS: Zn2+, that the band gap

energy values decrease while the concentration of Zn increases. It might be due to the lower band gap energy of ZnS compound i.e., band gap energy of ZnS is equal to 3.6eV [34].

The absorption spectra exhibit a shoulder around 515 nm (2.42 eV), resulting from the quantum confinement effect of Zn2+ doped CdS nanoparticles. It suggests a small blue shift of 0.03 eV of the absorption band from that of 505 nm (2.45 eV) for bulk CdS crystals at room temperature [35,36]. Thus, the band gap of Zn2+ doped CdS nanoparticles has been enlarged. Since the crystallite size of Zn2+ doped CdS nanoparticles is smaller than the Bohr radius of an exciton in bulk CdS crystal, a quantum confinement effect is expected to occur within these nanocrystals, exhibiting an enlargement of the optical band gap. Tuning the concentration of reactants was done to vary the growth rate at a particular instant of time. It is evident that the particle size decreases with increasing the Cds: Zn2+ ratio.

Figure (5) shows the overlay transmittance spectrum of CdS: Zn2+ (1 mol %, 2 mol % and 3mol %). The transmission spectra for CdS crystals in the wavelength range (300 - 2100 nm) are shown in Figure(5). All the crystals demonstrated more than 65% transmittance at wavelengths longer than 500 nm, which is comparable with the values for the CdS crystals deposited using the solvothermal method. Below 500 nm there was a sharp fall in the % T of the crystals, which was due to the strong absorbance of the crystals in this region. It has been observed that the overall % T decreases with Zn content.

The band gap energy of the doped samples is calculated by plotting the (% T) against λ and the obtained band gap energy values are given in table(3). It is evident from the values of the band gap energies for different ratio of CdS: Zn2+, that the band gap energy values increase while the concentration of Zn increases.

The absorption spectra of doped CdS nanoparticles with different concentration of Mn synthesized by microwave irradiation method are shown in figure(6). The presence of the absorption edge at ~490 nm is attributed to the characteristic absorption band edge of the CdS nanoparticles, which is blue-shifted from that of the corresponding bulk CdS. Additionally, a strong peak around 300nm is observed, which indicates the presence of tiny sized CdS nanoclusters [37]. The presence of localized magnetic ions in semiconductor alloys leads to exchange interactions between s-p band electrons of CdS and the Mn2+ electrons and plays a double role in determining optical properties (i) The band gap of the compound is altered depending upon the concentration of Mn ions. (ii) The 3d levels of Mn2+ ions are located in the band gap region and d-d transition dominates the spectrum. The absorption spectra of Mn doped CdS have similar features in comparison with the pure nanocrystalline CdS, but slightly red shifted indicating the quantum confinement effect. By increasing Mn content, a progressive slight red shift of about 0.1 eV has been observed. It is found that the red shift of the absorption threshold is almost consistent with the expected variation of the band gap for the bulk phase in the same Mn composition (from x = 0 to 0.3). The red shift of Mn2+ shows the variations in optical band gap and are given in table (4).

An absorption shoulder is observed at 470 nm in sample (a) , at 485 nm in sample (b) and at 495 nm in sample (c) for CdS nanoparticles synthesized by microwave oven with the concentration of 1mol%, 2mol% and 3mol% of Mn2+ respectively. The absorption edge of the above nanoparticles is observed to shift towards longer wavelengths with decreasing energy from 2.30 eV to 2.27 eV. This small change in band gap suggests that there is direct energy transfer between the semiconductor excited states and the 3d levels of the Mn2+ ions, which are coupled by energy transfer processes.[38]. It is observed that the band gap energy values for different ratio of Mn2+ doped in CdS nanoparticles decrease as the concentration of Mn dopant increases. It might be due to the lower band gap energy of MnS compound i.e., band gap energy of MnS is equal to 3.02 eV [39].

The trasmitance spectrum of the Mn2+ doped sample is shown in the figure (7). From the plot , the band gap energies are calculated and are given in table (5). It is evident from the values of the band gap energies for different ratio of CdS:Mn2+, that the band gap energy values increase while the concentration of Mn increases.

In the figure (8) it shows that, the overlay spectra of CdS: Cu2+ is in three different ratios. These three different ratios are obtained in the figure(8) shows the band gap energy values of the Cu2+ doped CdS and the values are given in table (6). It is noticed that the band gap energies for different ratio of Cu2+ in CdS decrease while the concentration of Cu increases. It might be due to the low band gap energy of CuS compound i.e., band gap energy of CuS is equal to 1.21eV [40].

The overlay transmittance spectrum of CdS: Cu2+ (1 mol %, 2 mol % and 3 mol %) shown in the figure (9). In this figure the transmission spectra for as CdS crystals are having the wavelength range (300 - 2100 nm). All the crystals have more than 65% transmittance at wavelengths longer than 500 nm, which is comparable with the values for the CdS crystals deposited using the solvothermal method. Due to the strong absorbance of the crystals there was a sharp fall in the T of the crystals at below 500 nm. Here it is observed that with the content of Cu2+ the overall % T decreases. With increasing the doping concentration, band gap energy is also increased. The band gap energy of the doped samples can be calculated and the obtained band gap energy values are given in table (7). It is evident from the values of the band gap energies for different ratio of CdS: Cu2+ , that the band gap energy values increase while the concentration of Cu increases.

3.3 FT-IR spectroscopic studies of CdS and CdS: Tm (Tm = Zn2+, Mn2+, Cu2+)

The phase purity and the presence of functional groups of the as-prepared pure Cds and CdS:Tm nanoparticles synthesized by the present solvothermal method are analysed using FT-IR spectroscopy.

The Infrared spectra of the samples are recorded in the range 400-4000 cm-1 on a Thermo-Nicolet Avatar 370 Fourier Transform Infrared (FT-IR) spectrometer. The powder samples are finely dispersed in KBr using an agate mortar and ground well. The finely dispersed materials are then pressed in the form of circular discs of nearly 10 mm diameter and 0.5 mm thickness at a pressure of 250 MPa. These pellets are then dried with IR light before the FT-IR spectra has been recorded.

The FTIR spectrum of pure CdS is shown in the figure (10) and the band assignment are given in the table (8). In the higher energy region the peak at 3426 cm-1 is assigned to O-H stretching of absorbed water on the surface of CdS [41]. The presence of water is confirmed by very weak bending vibration at 1616 cm-1, C-C stretching [42]. CdS particles showed two stretching bands, asymmetric and symmetric, the peak at around 2926 cm-1 is associated with C-H stretching. Medium strong band positions in the range of 1397 cm-1, is possibly due to stretching vibrations of sulphate group, shows the presence of thioacatamide[43] . The peak at 1114 cm-1 is assigned to C-O stretching vibration of ethylene glycol. There is a medium absorption band at 616 cm-1 has been assigned to C-H bending [44].

The FT-IR spectra of the as-prepared CdS doped with Zn2+, Mn2+, Cu2+ for 1 mol%, 2mol% and 3 mol% concentrations are shown in the figures 11-19 and vibrational assignments obtained in the spectra are given in the table (9). These exists only small variation in the wave numbers of different bands.

4. Conclusion

CdS nanoparticles have been synthesized by the microwave assisted solvothermal method. X-ray Diffraction (XRD) measurement conforms the structure of the CdS, having both cubic as well as hexagonal and the particle size is given by 16.65nm. The optical spectral studies of absorbance and transmittance mode are compared and studied. In the Uv-Vis absorbance mode, due to the quantum conferment of the charge carriers, the band gap energy of the pure CdS nanoparticles is increased by 0.03eV. But in the cause of Uv-Vis transmittance mode the band gap energy of the CdS nanoparticle is decreased by 0.12eV. From the FTIR spectra all the vibrational assignments are discussed.

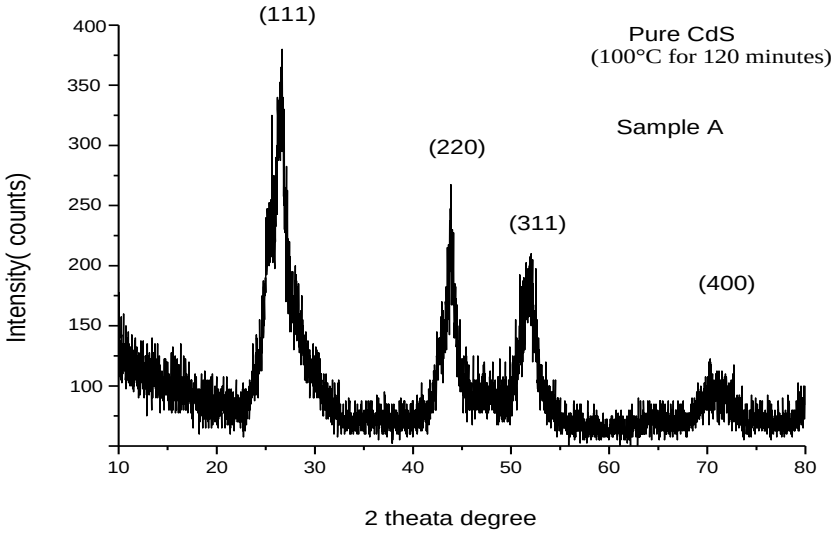

Fig: 1 XRD Of Pure CdS

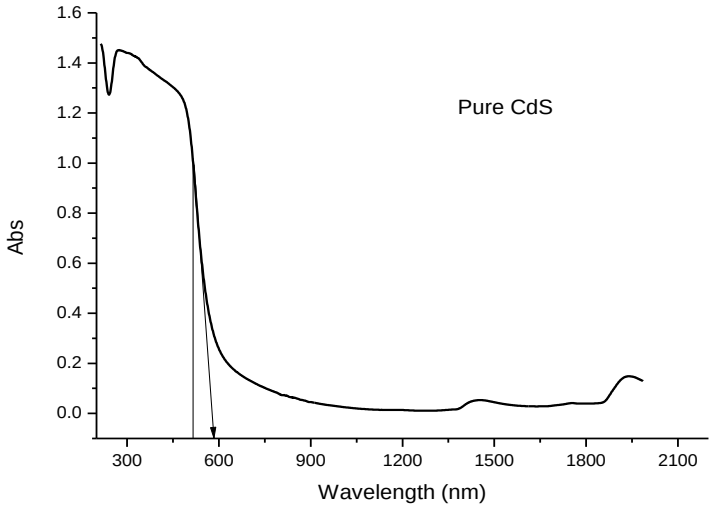

Fig:2 UV-VIS absorption spectrum

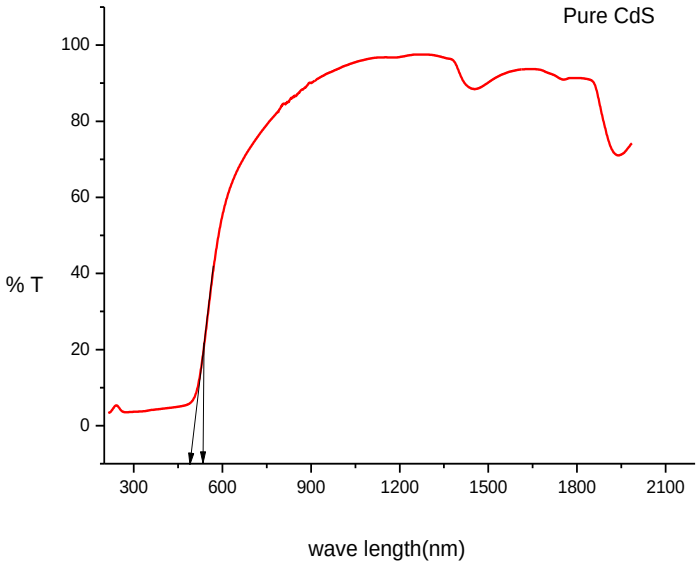

Fig :3 UV-VIS Transmittance spectrum

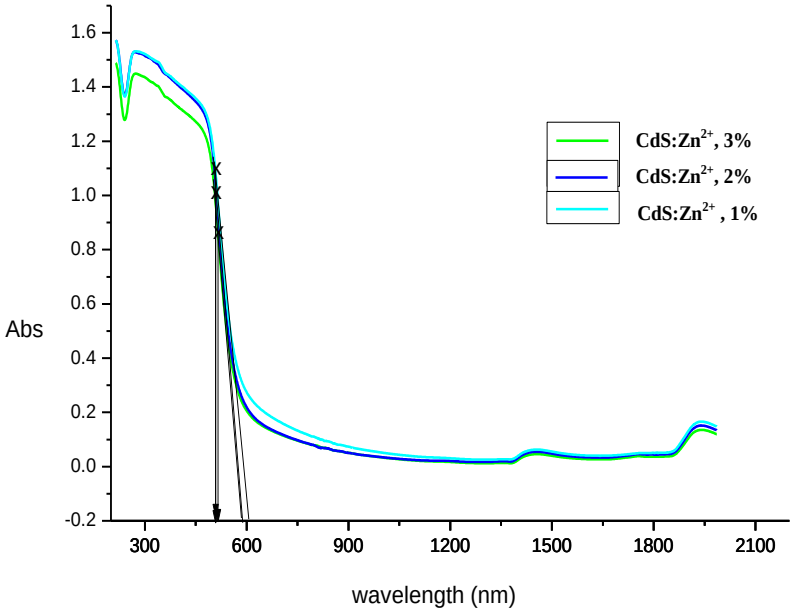

Fig:4 UV-VIS Abs. spectrum CdS:Zn2+

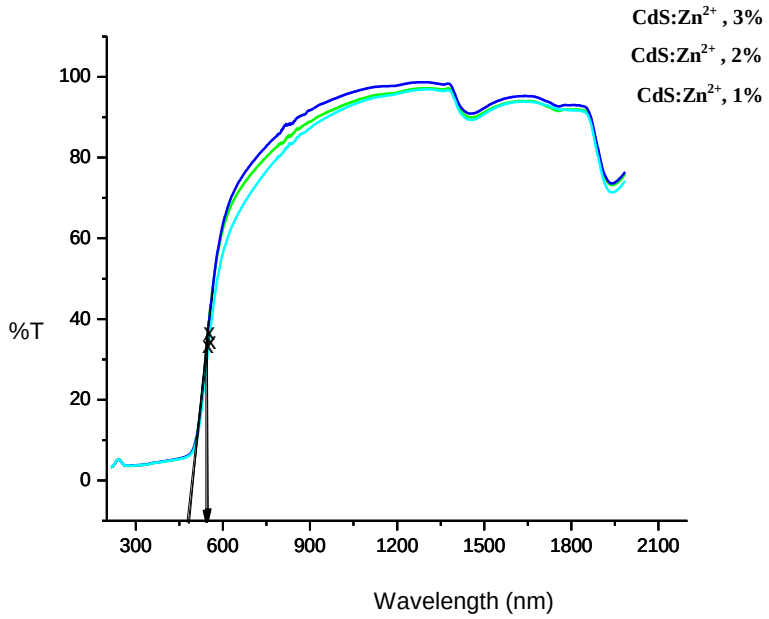

Fig:5 UV-VIS Trns. spectrum of of CdS: Zn2+

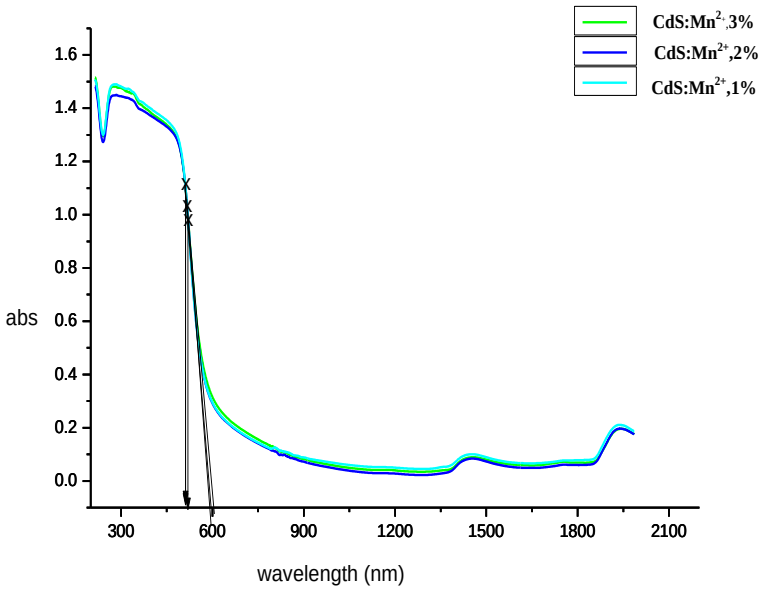

Fig: 6 UV-VIS Abs. spectrum CdS:Mn2+

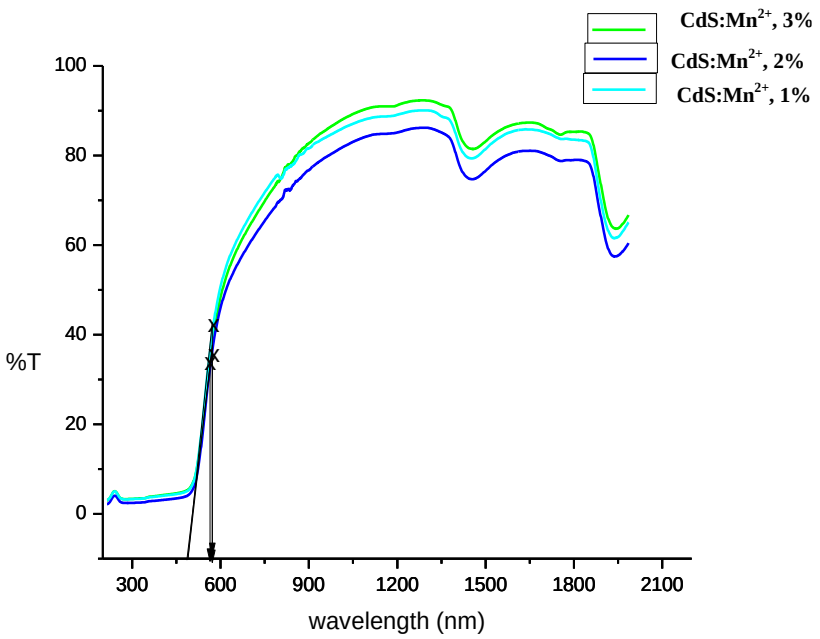

Fig:7 UV-VIS Trns. spectrum CdS:Mn2+

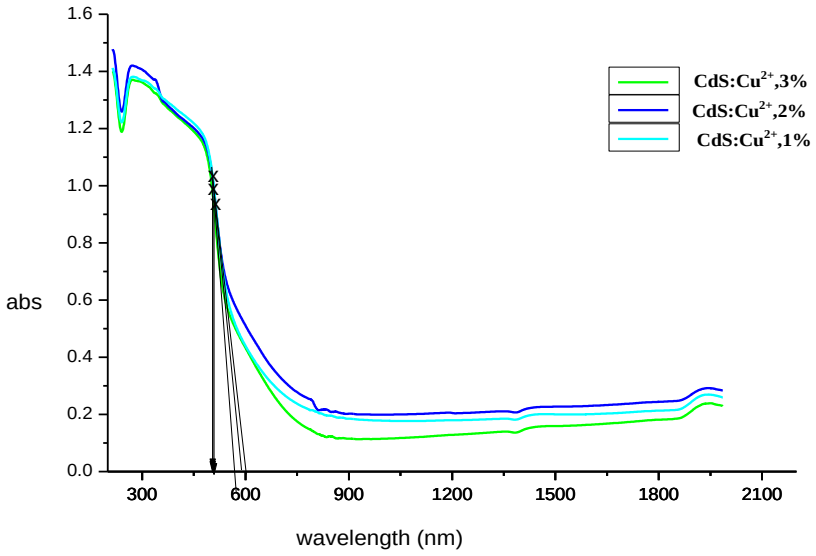

Fig: 8 UV-VIS Abs. spectrum CdS:Cu2+

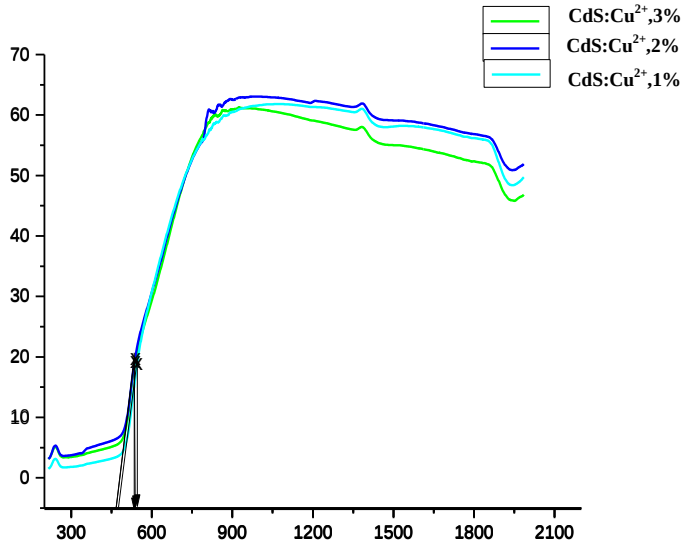

Fig: 9 UV-VIS Trns. spectrum CdS:Cu2+

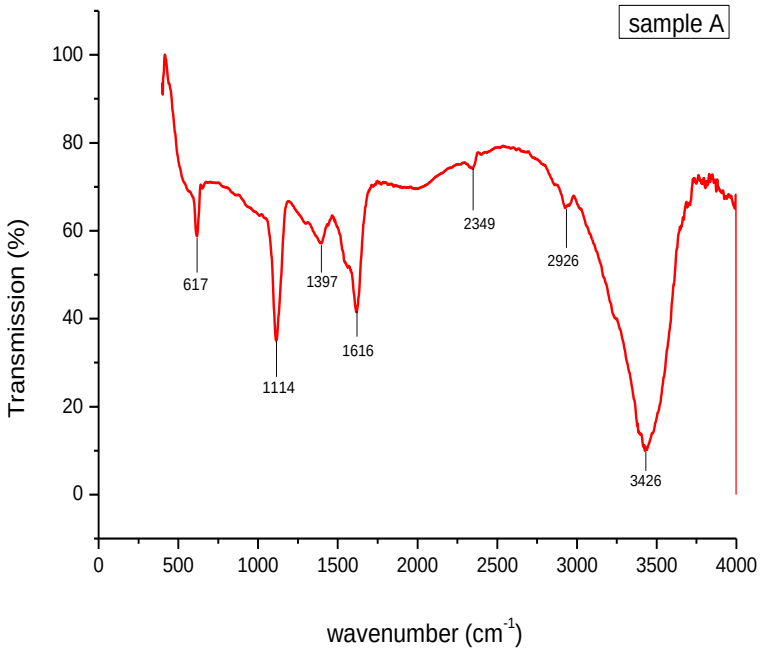

Fig:10 FTIR spectrum for pure CdS

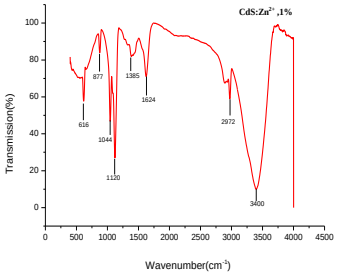

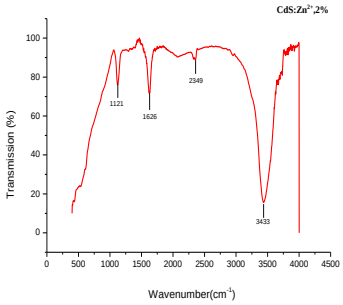

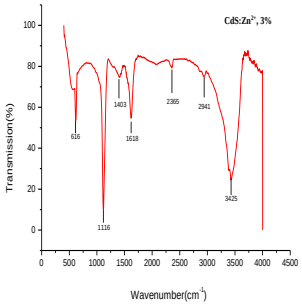

Fig: 11 **Fig:12** **Fig:13**

Fig(11- 13) FT-IR for CdS:Zn2+ (1 mol %, 2 mol % , 3 mol %)

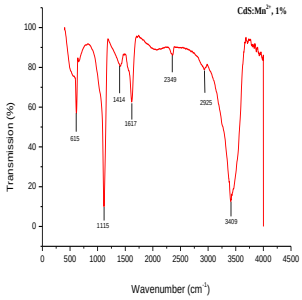

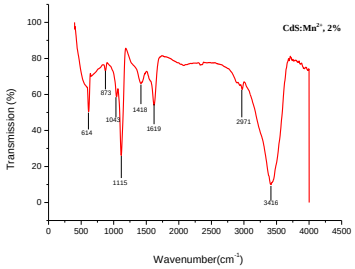

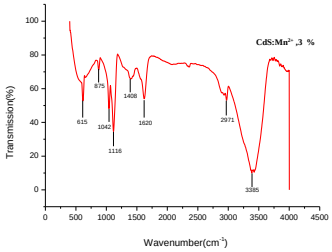

Fig: 14 **Fig: 15** **Fig: 16**

Fig:(14- 16) FT-IR for CdS:Mn2+ (1 mol %, 2 mol % , 3 mol %)

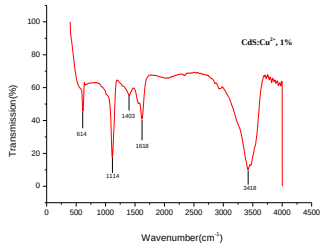

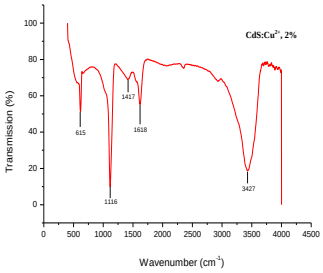

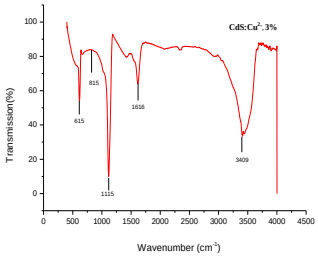

Fig: 17 **Fig: 18** **Fig: 19**

Fig:(17- 19) FT-IR for CdS:Cu2+ (1 mol %, 2 mol % , 3 mol %)

Experimental values		
(hkl)	**d-spacing Å**	**2θ (degrees)**
(111)	3.34	26.66
(220)	2.06	43.78
(311)	1.75	51.95
(400)	1.48	70.01

Table: 1 Eeperimental Value of XRD

Sample	**Particle size (nm)**	**(Eg) Band gap (eV)**
Cds (pure)	16.65	2.45
CdS:Zn2+(1 mol %)	14.49	2.44
CdS:Zn2+(2 mol %)	11.82	2.42
CdS:Zn2+ (3 mol %)	10.28	2.40

Table: 2 Band gap energy values (Abs.)

Sample	**Particle size(nm)**	**(Eg) Band gap (eV)**
Cds (pure)	16.65	2.30
CdS:Zn2+ (1 mol %)	14.93	2.23
CdS:Zn2+(2 mol %)	14.o6	2.25
CdS:Zn2+ (3 mol %)	12.12	2.27

Table: 3 Band gap energy values (Trns.)

sample	**Particle size (nm)**	**(Eg) Band gap (eV)**
Cds (pure)	16.65	2.45
CdS:Mn2+ (1 mol %)	14.93	2.43
CdS:Mn2+(2 mol %)	14.06	2.40
CdS:Mn2+ (3 mol %)	12.12	2.38

Table: 4 Band gap energy values (Abs.)

Sample	**Particle size (nm)**	**(Eg) Band gap (eV)**
Cds (pure)	16.65	2.30
CdS:Mn2+ (1 mol %)	14.93	2.15
CdS:Mn2+(2 mol %)	14.06	2.17
CdS:Mn2+ (3 mol %)	12.12	2.18

Table: 5 Band gap energy values (Trns.)

sample	**Particle size (nm)**	**(Eg) Band gap (eV)**
Cds (pure)	16.65	2.45
CdS:Cu2+ (1 mol %)	15.85	2.47
CdS:Cu2+(2 mol %)	13.31	2.45
CdS:Cu2+ (3 mol %)	12.78	2.43

Table: 6 Band gap energy values (Abs.)

Sample	**Particle size(nm)**	**(Eg) Band gap (eV)**
Cds (pure)	16.65	2.30
CdS:Cu2+ (1 mol %)	15.85	2.27
CdS:Cu2+(2 mol %)	13.31	2.29
CdS:Cu2+(3 mol %)	12.78	2.32

Table: 7 Band gap energy values (Trns.)

Sl. No	Wave number cm-1	Band assignment
1	3426	O-H Stretching
2	2926	C-H Stretching
3	2349	CH3 Stretching
4	1616	C-C Stretching
5	1397	S=O Sulphate group
6	1114	C-O Stretching
7	617	C-H Bending

Table:8 Vibratinal Assignments of Pure CdS

Sl. No	Wave number Cm-1 for				Band assignment
	Pure	1mol%	2mol%	3mol%	
1	3426	3400	3433	3425	O-H Stretching
2	2926	2972	-	2941	C-H Stretching
3	2349	-	2349	2365	CH3 Stretching
4	1616	1624	1626	1618	C-C Stretching
5	1397	1385	-	1403	S=O Sulphate group
6	1114	1120	1121	1116	C-O Stretching
7	616	616	-	616	SO4- Stretching

Table:9. Vibrational Assignments of pure and doped CdS nanoparticles

References

[1] Q. Wang, G. Xu, G. Han, J. Solid State Chem. **178**, 2680 (2005).

[2] Q. Nie, Q. Yuan, W.Chen, J. Cryst, Growth **265**, 420 (2004).

[3] X. Ma, F. Xu, Z. Zhang, Mater. Res. Bull. **40**, 2180 (2005).

[4] Y. Wang, C. Y. To, D.H. L. Ng, Mater. Lett. **60,** 1151(2006).

[5] R. Romano, O. L. Alves, Mater. Res. Bull. **41**, 376(2006).

[6] Y. Yang, h. Chen, X. Bao, J. Cryst. Grow. **252**, 251 (2003).

[7] A. Morales-Acevedo, Solar Energy Materials and Solar cells **90**, 2213 (2006).

[8] V. Singh, P. Chauhan, Chalcogenide Letters **6**, 421 (2009).

[9] S. Prabahar, N. Suryanarayanan, D. Kathirvel, Chalcogenide letters **6**, 577(2009).

[10] j. H. Schon, O. Schenker, B. Batlogg, Thin Solid Filims **385**, 271 (2001).

[11] I. O. Oladeji, L. Chow, J. R. Liu, W. K. Chu, A. N. P. Bustamante, C. Fredricksen, A. F. Schulte, Thin Solid Films **359**, 154 (2000).

[12]. S. Rinu Sam, S. L. Rayar and P. Selvarajan, J. Chemical and Pharmaceutical Research, **7(3)**: 957-963,(2015).

[13]. S. Rinu Sam, S. L. Rayar and P. Selvarajan, Int. J. Advanced Scientific and Technical Research, 5**(1)**, 198-207, (2015).

[14]. C. L. Cahill, B. Gugliotta and J . B. Parise, *Chem.Commun*. **16** (1998) 1715.

[15]. M. Schur, and W. Bensch, , *Z. Anorg. Allg. Che.* **624** (1998) 310.

[16]. G. C. Guo, R. M. W. Kwok and T. C. W. Mak, *Inorg.Chem. Soc.* **36** (1997) 2475.

[17]. C. Reisner and W. Tremel, *Chem.Commun*. **4** (1997) 387.

[18]. Y. Li, Y. Ding, Y. Qian, Y. Zhang and L. Yang, *Inorg. Chem*. **37** (1998) 2844.

[19]. J. Hu, Q. Lu, K. Tang, Y. Qian, G. Zhou and X. Liu, *Chem.Commun*. **12** (1999) 1093.

[20]. X. Qian,X. Zhang, C. Wang, Y. Xie and Y. Qian, *Inorg.Chem.* **38** (1999) 2621.

[21]. W. Wang, Y. Geng, P. Yan, F. Liu, Y. Xie and Y. Qian, *J Am.Chem. Soc.* **121** (1999) 4062.

[22]. W. Wang, P. Yan, F. Liu, Y. Xie, Y. Geng and Y. Qian, *J Mater.Chem.* **8** (1998) 2321.

[23]. S. Yu, J. Yang, Y. Wu, Z. Han, J. Lu, Y. Xie and Y. Qian, *ibid.* **8** (1998) 1949.

[24]. W. Horst, *Ang. Chem. Int. Ed. Engl*. **32** (1993) 41.

[25] Y. Li, H. Liao, Y. Fan, L. Li and Y. Qian, *Mater. Chem. Phys*. **58** (1999) 87.

[26] D. D. Papakonstantinou, J. Huang, P. Lianos, J. Mater. Sci. Lett., vol.17 (1998), 1571.

[27] W. Xu, Y. Wang, R. Xu, S. Liang, G. Zung, D. Yin, J. Matter. Sci., vol.**42** (2007), 6942.

[28].B. Murray, D. J. Norris,M. G. Bawendi, J. Am. Chem. Soc., vol.115 (1993), 8706.

[29]W.Wang, I. Germanenko, M. S. El Shall, Chem. Mater., vol.14 (2003), 3028.

[30] P. H. Borse, N. Deshmukh, R. F. Shinde, S. K. Date, S. K. Kulkarni, J. Mater. Sci.,vol.34 (1999) 6087.

[31]S. Liu, H. Zhang, M.T. Swihart, Nanotechnology, vol.20 (2009) 235603.

[32]X. W. Zhao, S. Komuro, S. Fujita, H. Isshiki, Y. Aoyagi, T. Sugano, Mat. Sci.Eng., B vol.51(1998), 154.

[33] M. Kamruzzaman, T. R. Luna, J. Podder , Innvat. Sys. Des. Engg., vol.2a, no 5, (2011).

[34] S.N. Agbe, F.I. Ezema, Pacific Journal of Science and Technology., vol.8 (2007).

[35]R.N. Bhargava, D. Gallagher, T. Welker, J. Lumin., vol.60 (1994), 275.

[36] R.N. Bhargava, D. Gallagher, X. Hong, A. Nurmikko, Phys. Rev. Lett., vol.72 (1994) 416.

[37] G.S. Harish, A. Divya, K. Siva Kumar and P. Sreedhara Reddy Res. J. Physical Sci ISSN 2320–4796 Vol. 1(7), 7-10, August (2013).

[38] S.M. Agbel, F.I. Elzema, Pacific Journal of Science and Technology, 8 (2007)1.

[39] D. O. Papakonstantinou, G. Huang, P. Lianos, J. Mater. Sci. Lett. 17 (1998) 1571.

[40] R.S. Mane, C.D. Lokhande, Mater.Chem. Phys., vol.78 (2003), 15.

[41] C. Yohannan Panikcker, Hema Tresa Varghese, Daizy Philip, spct. Acta . Mol. Bio mol. Specpy.,vol.65 (2006), 802-805.

[42] B. Sreenivasa Rao, B. Rajesh Kumar, V. Rajagopal Reddy, T. Subba Rao,chl.Let., vol. 8 (2011), 177-185.

[43] A.Aneeqa Sabha, Saadat Anwar Siddiqi, Salamat Ali, Wld. Acdmy. of Scin.Engg and Tech., vol.45, 2010.

[44] P. Venkatesu, K. Ravichandran, Adv. Mat. Lett., vol.4(3)(2013), 202-206.